JOURNAL OF SOLID STATE CHEMISTRY **127,** 231–239 (1996)
ARTICLE NO. 0379

Lanthanide-Containing Zirconotitanate Solid Solutions[1,2]

Shara S. Shoup, Carlos E. Bamberger,[3] Jennifer L. Tyree,[4] and Lawrence M. Anovitz

Chemical and Analytical Sciences Division, Oak Ridge National Laboratory, Oak Ridge, Tennessee 37831–6119

Received February 12, 1996; in revised form June 21, 1996; accepted September 10, 1996

Solid solutions between several lanthanide-containing dititanate and dizirconate compounds have been synthesized and identified using X-ray diffraction (XRD). Complete solubility was found in the pyrochlore–pyrochlore-type systems $Er_2Ti_2O_7$–$Nd_2Zr_2O_7$ and $Nd_{1.2}Er_{0.8}Ti_2O_7$–$Nd_2Zr_2O_7$. Some solubility of $Nd_2Ti_2O_7$, a monoclinic dititanate, in defect fluorite $Er_2Zr_2O_7$ was observed, and it was determined that there is some solubility of $Nd_2Ti_2O_7$ in pyrochlore-type $Nd_2Zr_2O_7$. The systems $Nd_2Zr_2O_7$–TiO_2 and $Nd_2Ti_2O_7$–ZrO_2 also were investigated to help define a region of pyrochlore solid solution formation in the system $NdO_{1.5}$-TiO_2-ZrO_2. Additionally, attempts were made to synthesize pyrochlore-type solid solutions between $Ce_2Ti_2O_7$ and $Ce_2Zr_2O_7$ and to substitute titanium with zirconium in the perovskite-type phases $SrNd_2Ti_4O_{12}$ and $Sr_2Ce_2Ti_5O_{16}$.

INTRODUCTION

The symmetry of the lanthanide dititanates changes as a function of the atomic number of the lanthanide element. The lanthanide dititanates ($Ln_2Ti_2O_7$) from lanthanum to neodymium are monoclinic (1), whereas the dititanates from samarium to lutetium ($Ln'_2Ti_2O_7$) exhibit a cubic pyrochlore-type structure (2). Similarly, the lanthanide dizirconates do not all exhibit the same crystal structure. From lanthanum to gadolinium, they adopt a cubic pyrochlore-type structure (2). The remaining lanthanide dizirconates, which have radius ratios too small for pyrochlore formation, exhibit a defect fluorite structure (2). In both systems the formation of pyrochlore structures requires radius ratios $1.46 \leq r_{Ln^*}/r_{\mathrm{Ti\ or\ Zr}} \leq 1.78$, where r_{Ln^*} and $r_{\mathrm{Ti\ or\ Zr}}$ are the ionic radii of, respectively, any lanthanide, titanium, and zirconium.

The existence of multisubstituted pyrochlores has been well established, and there are many examples of such lanthanide-containing compounds in the literature (3–5). The formation of pyrochlore solid solutions between $Ln_2Ti_2O_7$ and $Ln'_2Ti_2O_7$ has been investigated and solid solubility limits of several $Ln_2Ti_2O_7$ in $Ln'_2Ti_2O_7$ have been established (4, 5); however, few solid solutions between pyrochlore-type titanates and zirconates have been investigated. One example is the system $Gd_2Ti_2O_7$–$Gd_2Zr_2O_7$, which shows complete miscibility between the two pyrochlores (6). A series of solid solutions $Y_2(Zr_nTi_{1-n})_2O_7$ was reported in which the structure changed from pyrochlore type to defect fluorite with increasing zirconium content (7); however, small amounts of a fluorite-like phase, increasing with zirconium content, were present along with the solid solution at all compositions (7), indicating that the compositions assigned to the solid solutions were not correct.

There are few known lanthanide-bearing titanates that exhibit the perovskite structure. Solid solution formation between $Ln_2Ti_3O_{9-3m}$ (Ln = La–Nd, $m < 0.25$) and the cubic perovskite $SrTiO_3$ has been examined (8). The resulting solid solutions have the composition $Sr_{4-x}Ln_{2x/3}Ti_4O_{12}$ ($0 \leq x \leq 4$), where the lanthanide ion is trivalent. Another series of perovskite-type solid solutions studied is that of $Sr_{6-12x}Ce_{6x}Ti_5O_{16}$ ($0.08 \leq x \leq 0.43$), where cerium is tetravalent (9). There are also a few known mixed titanium–zirconium compounds or solid solutions which exhibit perovskite-type structures, although in the sodium-containing system $Na_{0.5}La_{0.5}Ti_{1-x}Zr_xO_3$ ($Na_2La_2Ti_{4-y}Zr_yO_{12}$, $y = 4x$), perovskite-type solid solutions reportedly form at all compositions (10).

The lanthanide-containing pyrochlore and perovskite solid solutions have interesting dielectric properties (11) and are also potential hosts for immobilizing nuclear waste. Zirconium-containing minerals, such as tetragonal zircon ($ZrSiO_4$) (12), monoclinic zirconolite ($CaZrTi_2O_7$) (13–17), and synthetics such as $La_2Zr_2O_7$ (18), are being explored as possible matrices for radionuclides from spent nuclear fuel, medical and research waste, waste generated by the weapons program, and the dismantling of nuclear weapons. Zircon is found in nature immobilizing uranium

[1] Adapted from a dissertation submitted by S. S. Shoup in partial fulfillment of the requirements for the Ph.D. degree in Chemistry from the Department of Chemistry, University of Tennessee, Knoxville.

[2] The U.S. Government's right to retain a nonexclusive royalty-free license in and to the copyright covering this paper, for governmental purposes, is acknowledged.

[3] To whom correspondence should be addressed.

[4] Science Alliance Summer Research Participant, University of Tennessee, Martin, TN.

0022-4596/96 $18.00

and thorium (19). Zirconolite is one of the minerals present in SYNROC (13, 14), a synthetic ceramic also containing perovskite ($CaTiO_3$) and hollandite ($BaAl_2Ti_6O_{16}$) that seeks to mimic minerals which, like zircon, are geologically stable and have retained naturally occurring radioactive elements for millions of years. $La_2Zr_2O_7$ exhibits the pyrochlore-type structure which is also potentially suitable for immobilizing nuclear waste (20). An advantage of these compounds and minerals is that they can accommodate many elements, covering a wide range of ionic sizes and valences, in their structures by substitution. This is an important consideration for immobilizing the many elements present in high-level radioactive waste.

The first step in establishing the possible utility of these types of compounds and solid solutions as possible waste hosts for actinides is to define the existence and the limits of solid solution. Since, based on the corresponding ionic radii and electronic structures, it is accepted that lanthanide elements can be used as surrogates for actinides, lanthanide elements are used here in that capacity. The lack of information pertaining to zirconotitanate systems motivated our interest, but because of the multiple structures they exhibit, only a few representative systems are studied here. The systems $Er_2Ti_2O_7$–$Nd_2Zr_2O_7$ and $Nd_{1.2}Er_{0.8}Ti_2O_7$–$Nd_2Zr_2O_7$ were chosen for studying pyrochlore–pyrochlore-type solid solutions containing titanium and zirconium. As an example of phase relations between other structures in the system, the solubility of monoclinic $Nd_2Ti_2O_7$ in defect fluorite $Er_2Zr_2O_7$ and the solubility of monoclinic $Ce_2Ti_2O_7$ and $Nd_2Ti_2O_7$ in pyrochlore-type dizirconates containing the same lanthanide were also examined. The systems $Nd_2Zr_2O_7$–TiO_2 and $Nd_2Ti_2O_7$–ZrO_2 were examined to determine the extent of pyrochlore-type solid solution formation and to help define a region of solid solubility in the $NdO_{1.5}$–TiO_2–ZrO_2 ternary system. The possibility of replacing some of the titanium with zirconium in the perovskite-type compounds $SrNd_2Ti_4O_{12}$($Sr_{4-x}Nd_{2x/3}Ti_4O_{12}$, $x = 3.0$) and $Sr_2Ce_2Ti_5O_{16}$ ($Sr_{6-12x}Ce_{6x}Ti_5O_{16}$, $x = 0.333$) was also explored.

EXPERIMENTAL PROCEDURES

Starting mixtures were prepared by dry grinding together the required amounts of the corresponding oxides (CeO_2, Nd_2O_3, Er_2O_3, TiO_2, ZrO_2) and $SrCO_3$ when appropriate. These reactants were at least 99% pure except for Nd_2O_3, which was labeled 95% pure with respect to the lanthanide element. The Nd_2O_3 was either dried in air between 900 and 1050°C for a minimum of 4 h or used without drying but compensating in mass for its moisture content. TiN or ZrN was added to the mixture in stoichiometric amounts to reduce Ce(IV) to Ce(III) in the presence of TiO_2 (5) and/or ZrO_2, for example,

$$2CeO_2 + 0.5ZrN + 1.5ZrO_2 \rightarrow Ce_2Zr_2O_7 + 0.25N_2. \quad [1]$$

The mixtures, in the form of pellets, were placed in Al_2O_3 or Pt boats for all or at least the final heat treatments. The cerium-containing mixtures were reacted in Ar or Ar–4% H_2 between 1200 and 1450°C, whereas the other lanthanide-bearing mixtures were reacted in air between 1350 and 1500°C. The weight changes associated with all the thermal treatments were recorded and rationalized. Reaction times varied from 30 to 325 h with as many as six regrindings between firings until no changes in composition were seen by XRD. The cerium-containing compounds were allowed to cool slowly to room temperature, typically overnight, under the atmosphere in which they had been reacted, Ar or Ar–4% H_2, whereas the other lanthanide-bearing compounds were cooled rapidly in air.

It was noted that the point at which no more changes were detected was harder to achieve in the mixed titanium–zirconium systems than in the titanium-only systems (4, 5, 8, 9).

Resultant compounds and solid solutions were identified and characterized by XRD. The fine-grained (1–5 μm) nature of the reaction products was not conducive to the use of electron microprobe analysis to quantify the composition of the various phases. XRD data were collected using a diffractometer (Bragg–Brentano) equipped with a theta-compensating incident beam divergence slit and a graphite (002) diffracted beam monochromator. Cu$K\alpha_1$ radiation was utilized, and the scan rate was 1.2°/min. The samples were thinly coated on ''zero-background'' silicon substrate plates and were approximately 30 mg in mass. Silicon powder (a_0 = 0.53406 nm) was used as an external standard to periodically calibrate the diffractometer.

Pattern-processing software (Jade, Materials Data Inc., Livermore, CA, 1994) was used to strip $K\alpha_2$ and locate peaks in the XRD data. A least-squares program, LATTICE (21), was used to calculate lattice parameters.

RESULTS AND DISCUSSION

Pyrochlore-Type Solid Solutions in the Systems $Er_2Ti_2O_7$-$Nd_2Zr_2O_7$ and $Nd_{1.2}Er_{0.8}Ti_2O_7$-$Nd_2Zr_2O_7$

In the system $Er_2Ti_2O_7$–$Nd_2Zr_2O_7$, where both end-member compounds exhibit cubic pyrochlore-type structures, cubic pyrochlore-type solid solutions ($Nd_{2-x}Er_x$)(Ti_xZr_{2-x})O_7 ($0 \le x \le 2$) formed at any value of x. The formula unit volume[5] ($Z = 8$) varied linearly with composition (Fig. 1).

The system $Nd_{1.2}Er_{0.8}Ti_2O_7$–$Nd_2Zr_2O_7$ was also examined for solid solution formation because $Nd_{1.2}Er_{0.8}Ti_2O_7$ is a neodymium-bearing, pyrochlore-type solid solution on the join between monoclinic $Nd_2Ti_2O_7$ and pyrochlore-

[5] Formula unit volume = unit cell volume/Z, where Z = number of formula units in unit cell.

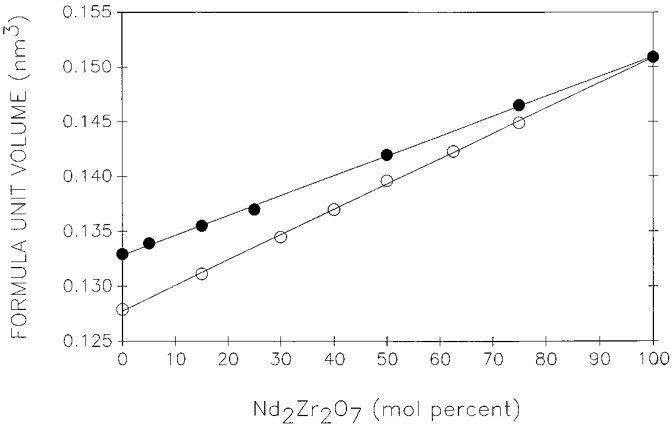

FIG. 1. Measured formula unit volume of $(Nd_{2-x}Er_x)(Ti_xZr_{2-x})O_7$ (○) and $(Nd_{2-x}Er_x)(Ti_{2.5x}Zr_{2-2.5x})O_7$ (●) versus mole percent of $Nd_2Zr_2O_7$ in the initial mixture. The errors for the data points are smaller than the height of the symbols.

type $Er_2Ti_2O_7$ (4). Complete miscibility was found in the $Nd_{1.2}Er_{0.8}Ti_2O_7$–$Nd_2Zr_2O_7$ system, and all of the compounds formed were pyrochlores. These solid solutions have the generalized formula $(Nd_{2-x}Er_x)(Ti_{2.5x}Zr_{2-2.5x})O_7$ ($0 \le x \le 0.8$). The measured formula unit volume ($Z = 8$) of the solid solution increased linearly with increasing mole percentage of the larger $Nd_2Zr_2O_7$ in the mixture (Fig. 1). The compositions and volumes measured for preparations in the systems $Er_2Ti_2O_7$–$Nd_2Zr_2O_7$ and $Nd_{1.2}Er_{0.8}Ti_2O_7$–$Nd_2Zr_2O_7$ are given in Table 1.

Pyrochlore-Type Solid Solution Formation in the System $Nd_2Ti_2O_7$-$Er_2Zr_2O_7$

The system $Nd_2Ti_2O_7$–$Er_2Zr_2O_7$ is the reciprocal of $Er_2Ti_2O_7$–$Nd_2Zr_2O_7$ discussed above; however, $Nd_2Ti_2O_7$ exhibits monoclinic symmetry, whereas $Er_2Zr_2O_7$ has a defect fluorite-type structure to which $Z = 1$ was assigned (2). XRD analysis of preparations containing 25 to 75 mol% $Nd_2Ti_2O_7$ indicated that they consisted of single-phase pyrochlore-type solid solutions. The formula unit volume ($Z = 8$) of the solid solution decreased with increasing mole percentage of $Nd_2Ti_2O_7$. Significant apparent excess volume is observed (Fig. 2); this can be rationalized on the basis that two phase transformations, rather than one, occur along the $Nd_2Ti_2O_7$–$Er_2Zr_2O_7$ join: defect fluorite ($Er_2Zr_2O_7$) → pyrochlore ($Er_2Zr_2O_7$–$Nd_2Ti_2O_7$ solid solutions) → monoclinic ($Nd_2Ti_2O_7$). While the exact compositions at which these phase transformations occur are not accurately known, they can be estimated based on the XRD data. The transformation from defect fluorite to pyrochlore is estimated to occur around 25 mol% $Nd_2Ti_2O_7$ because the resulting solid solution is a pyrochlore-type that has nearly the expected volume based on Vegard's law. A two-phase region may already exist at this boundary, however; we were not able to ascertain this with only XRD because the diffraction patterns of these fluorite and pyrochlore structures overlap considerably. The phase boundary between pyrochlore and monoclinic phases must occur at greater than 75 mol% $Nd_2Ti_2O_7$ because no monoclinic phase was observed at this composition. Previous results with lanthanide dititanate pyrochlore–monoclinic joins (4, 5) suggest that indeed a two-phase region occurs between 75 and 100 mol% $Nd_2Ti_2O_7$.

Pyrochlore-Type Solid Solutions in the System $Nd_2Ti_2O_7$-$Nd_2Zr_2O_7$

Cubic pyrochlore-type solid solutions $Nd_2Zr_{2-x}Ti_xO_7$ were found to exist up to $x \approx 0.86$ in the system $Nd_2Ti_2O_7$–$Nd_2Zr_2O_7$. The formula unit volumes ($Z = 8$) decreased linearly from 0 to 43 mole% $Nd_2Ti_2O_7$ (Fig. 3). At this composition the function changed slope. For greater $Nd_2Ti_2O_7$ concentrations, the volume of the solid solution remained fairly constant and a monoclinic phase, consistent with $Nd_2Ti_2O_7$, was detected by XRD in addition to the pyrochlore. The deviation from constant formula unit volume of the saturated pyrochlore very likely reflects the effect of overlap of monoclinic and pyrochlore diffraction lines. This can affect the precision of the formula unit volume determination.

Figure 4 summarizes phase equilibria in the system $(Nd,Er)_2(Ti,Zr)_2O_7$ determined from our results on the joins: $Er_2Ti_2O_7$–$Nd_2Zr_2O_7$, $Nd_{1.2}Er_{0.8}Ti_2O_7$–$Nd_2Zr_2O_7$, $Nd_2Ti_2O_7$–$Er_2Zr_2O_7$, and $Nd_2Ti_2O_7$–$Nd_2Zr_2O_7$. The dotted lines represent, very approximately, the phase transformation boundaries (e.g., from defect fluorite to pyrochlore). The dashed line represents the beginning of a two phase (pyrochlore and monoclinic) region determined from this work along the $Nd_2Ti_2O_7$–$Nd_2Zr_2O_7$ join and from previous work along the $Nd_2Ti_2O_7$–$Er_2Ti_2O_7$ join (4). Although a two-phase region between defect fluorite and pyrochlore may exist, it is not shown because sufficient data are not available.

Pyrochlore-Type Solid Solutions in the Reciprocal Systems $Nd_2Zr_2O_7$–TiO_2 and $Nd_2Ti_2O_7$-ZrO_2

Up to approximately 0.56 mol of TiO_2 was soluble in 1 mol of $Nd_2Zr_2O_7$ ($X_{TiO_2} = 0.12$),[6] forming a cubic pyrochlore-type solid solution. Additional TiO_2, up to approximately 1.5 mol per $Nd_2Zr_2O_7$ ($X_{TiO_2} = 0.27$), was incorporated into a pyrochlore-type solid solution, but ZrO_2 was exsolved as indicated by XRD data. When 2 mol of TiO_2 per $Nd_2Zr_2O_7$ ($X_{TiO_2} = 0.33$) was reacted, the separation of a ZrO_2 solid solution was detected. When 2.5 mol of TiO_2 per $Nd_2Zr_2O_7$ was reacted with $Nd_2Zr_2O_7$ ($X_{TiO_2} =$

[6] $X_{TiO_2} = n_{TiO_2}/(n_{TiO_2} + n_{ZrO_2} + n_{NdO_{1.5}})$, where n_i is the number of moles.

TABLE 1
Compositions and Formula Unit Volumes of the Pyrochlore-Type Solid Solutions Found in the Systems $Er_2Ti_2O_7$–$Nd_2Zr_2O_7$ and $Nd_{1.2}Er_{0.8}Ti_2O_7$–$Nd_2Zr_2O_7$

$Er_2Ti_2O_7$–$Nd_2Zr_2O_7$

Composition (mol%)		Formula unit volume
$Er_2Ti_2O_7$	$Nd_2Zr_2O_7$	(nm^3)
0	100	0.1509
25	75	0.1449
37.5	62.5	0.1423
50	50	0.1396
60	40	0.1370
70	30	0.1345
85	15	0.1311
100	0	0.1279

$Nd_{1.2}Er_{0.8}Ti_2O_7$–$Nd_2Zr_2O_7$

Composition (mol%)		Formula unit volume
$Nd_{1.2}Er_{0.8}Ti_2O_7$	$Nd_2Zr_2O_7$	(nm^3)
0	100	0.1509
25	75	0.1465
50	50	0.1420
75	25	0.1370
85	15	0.1355
95	5	0.1339
100	0	0.1329

0.38), the system was severely affected, and the XRD data from the preparation indicated the presence of $Nd_2Ti_2O_7$, a ZrO_2 solid solution, and a pyrochlore-type phase with a volume close to that of pure $Nd_2Zr_2O_7$. The formula unit volume ($Z = 8$) of the major phases along this join $Nd_2Zr_2O_7$–TiO_2 is a complex function (Fig. 5). The data can be fitted to a curve which may be interpreted as reflecting a continuous change in phases and composition. The corresponding XRD data, however, permit us to speculate that several reactions, represented by linear segments, take place as the TiO_2 increases. Three segments, A, B, and C, can be distinguished. The slope of the line for single-phase pyrochlore solid solutions is steep (segment A). This can be interpreted by means of the equations

$$Nd_2Zr_2O_7 + 0.24TiO_2 \rightarrow 1.07Nd_{1.87}Ti_{0.22}Zr_{1.87}\square_{0.03}O_7, \quad [2]$$

$$Nd_2Zr_2O_7 + 0.44TiO_2 \rightarrow 1.13Nd_{1.78}Ti_{0.39}Zr_{1.78}\square_{0.06}O_7. \quad [3]$$

In these equations and the subsequent ones below, the formulas of the products have been normalized to a content of seven oxygens assigned to the observed cubic pyrochlore phase. It has also been assumed that the titanium distributes equally between the neodymium and zirconium sites, yielding the exchange

$$Nd^{3+} + Zr^{4+} = 1.75Ti^{4+} + 0.25\square \quad [4]$$

in which the location of the vacancy is undetermined.

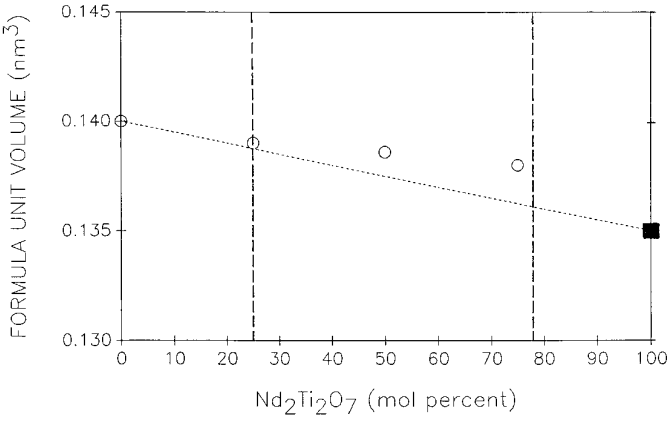

FIG. 2. Measured formula unit volume of pyrochlore-type solid solution between $Nd_2Ti_2O_7$ and $Er_2Zr_2O_7$ versus mole percent of $Nd_2Ti_2O_7$ in the initial mixture. The dotted line connects the volume of $Er_2Zr_2O_7$ with that of $Nd_2Ti_2O_7$ (■). Approximate phase transformation boundaries are marked with broken vertical lines. The errors for the data points are smaller than the height of the symbols.

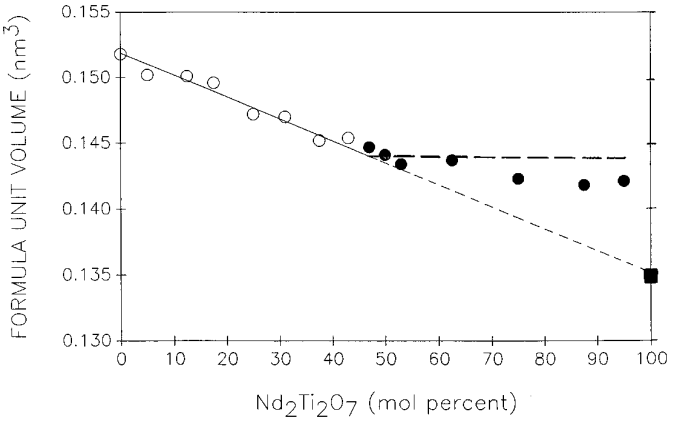

FIG. 3. Measured formula unit volume of $Nd_2Zr_{2-x}Ti_xO_7$ versus mole percent of $Nd_2Ti_2O_7$ in the initial mixture. The diagonal sloped line connects the volume of $Nd_2Zr_2O_7$ with that of $Nd_2Ti_2O_7$ (■). The horizontal line (filled symbols) indicates saturation of the host matrix with $Nd_2Ti_2O_7$. The errors for the data points are smaller than the height of the symbols.

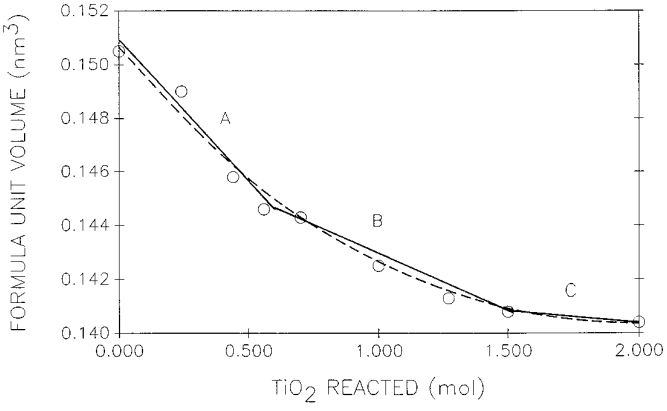

FIG. 5. Measured formula unit volume of pyrochlore-type solid solution between $Nd_2Zr_2O_7$ and TiO_2 versus the number of moles of TiO_2 reacted per mole of $Nd_2Zr_2O_7$. The curve reflects possible continuous change in phases and composition. A, B, and C denote three possible regions of linearity. The errors for the data points are smaller than the height of the symbols.

The appearance of ZrO_2 was first detected between 0.56 and 0.70 mol of TiO_2 and continued up to 1.5 TiO_2. This is represented by segment B, which has a slope not as steep as that for the single-phase pyrochlore. Taking arbitrarily the value of 0.62 mol TiO_2 per mole of $Nd_2Zr_2O_7$ as the limit above which ZrO_2 exsolves,

$$Nd_2Zr_2O_7 + 0.62TiO_2 \rightarrow 1.18Nd_{1.70}Ti_{0.53}Zr_{1.70}\square_{0.08}O_7, \quad [5]$$

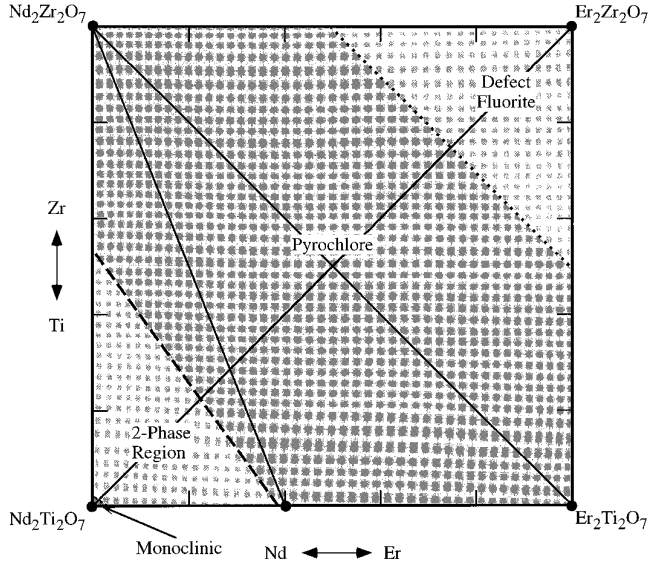

FIG. 4. Summary of the $(Nd,Er)_2(Ti,Zr)_2O_7$ system. · · ·, Very approximate phase transformation boundaries; ---, Two-phase (pyrochlore and monoclinic) region.

segment B can be interpreted as shown by

$$Nd_2Zr_2O_7 + 0.70TiO_2 \rightarrow 1.18Nd_{1.70}Ti_{0.59}Zr_{1.64}\square_{0.08}O_7 + 0.07ZrO_2, \quad [6]$$

$$Nd_2Zr_2O_7 + 1.27TiO_2 \rightarrow 1.18Nd_{1.70}Ti_{1.08}Zr_{1.15}\square_{0.08}O_7 + 0.64ZrO_2. \quad [7]$$

The above equations were derived by assuming that all the TiO_2 is incorporated and only ZrO_2 in excess of that needed to balance the charges is exsolved. This is consistent with the observation by XRD of the presence of ZrO_2 and pyrochlore.

A third linear region (segment C) occurs between 1.5 and 2 mol of TiO_2 reacted per mole of $Nd_2Zr_2O_7$ (X_{TiO_2} = 0.27 and 0.33). In this segment C, the volume of the solid solution does not change greatly with increasing TiO_2. This probably reflects the fact that the pyrochlore phase is saturated with TiO_2.

Several compositions were also investigated in the reciprocal system $Nd_2Ti_2O_7$–ZrO_2. Reaction of $Nd_2Ti_2O_7$ with varying amounts of ZrO_2 did not result in the formation of a single-phase compound. Instead, the XRD data indicated that a cubic pyrochlore-type compound and $Nd_2Ti_2O_7$ were present.

Phase Relations in the System $NdO_{1.5}$–TiO_2–ZrO_2

While the results of synthesis reactions such as those described for the system $NdO_{1.5}$–TiO_2–ZrO_2 in this paper do not prove that equilibrium has been achieved and no reversed reactions were performed in this study, the fact

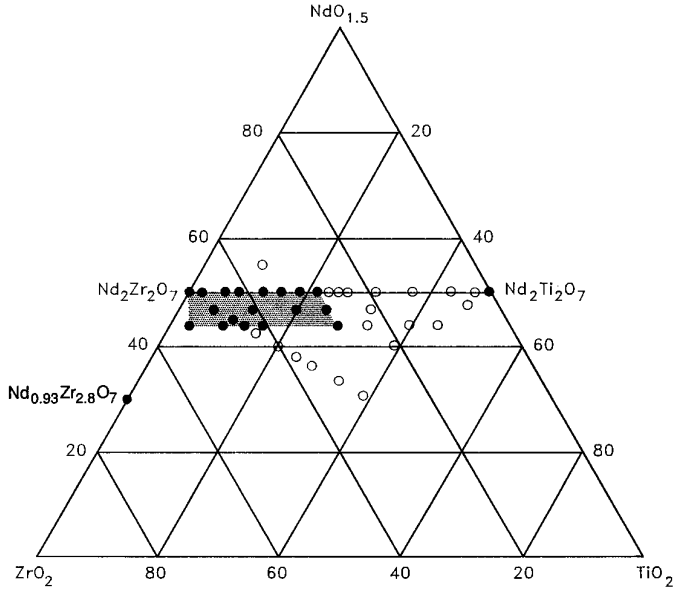

FIG. 6. Single-phase, pyrochlore-type solid solution region within the system $NdO_{1.5}$–TiO_2–ZrO_2 between 1400 and 1500°C. ●, Single phase; ○, more than one phase, Shaded area indicates a region of single-phase solid solution.

that all our compositions were repeatedly reacted and reground until no further changes in the XRD data were observed gives confidence that our final results represent the equilibrium state of the system.

Based on our data for the systems $Nd_2Ti_2O_7$–$Nd_2Zr_2O_7$, $Nd_2Zr_2O_7$–TiO_2, and $Nd_2Ti_2O_7$–ZrO_2 and additional compositions, a region of single-phase pyrochlore-type solid solutions was identified in the ternary system and is shown in Fig. 6. This region is relatively large and is limited by the following compositions: [50 mol% $NdO_{1.5}$, 50 mol% ZrO_2]; [50 mol% $NdO_{1.5}$, 21.5 mol% TiO_2, 28.5 mol% ZrO_2]; [43.9 mol% $NdO_{1.5}$, 4.1 mol% TiO_2, 52.0 mol% ZrO_2]; and [43.9 mol% $NdO_{1.5}$, 27.8 mol% TiO_2, 28.3 mol% ZrO_2]. An additional sample on the $NdO_{1.5}$–ZrO_2 binary (40 mol% $NdO_{1.5}$, and 60 mol% ZrO_2) also yielded a single-phase pyrochlore.

Combining our data for the $NdO_{1.5}$–TiO_2–ZrO_2 system with published work on the joins $NdO_{1.5}$–TiO_2 (22), $NdO_{1.5}$–ZrO_2 (23, 24), $NdO_{1.5}$–HfO_2 (25) (see below), and TiO_2–ZrO_2 (26) allows us to construct a tentative phase diagram for the $NdO_{1.5}$–TiO_2–ZrO_2 system at 1400–1500°C (Fig. 7). A number of phases occur on the $NdO_{1.5}$–TiO_2 binary. In this temperature range, data for this join and $NdO_{1.5}$–ZrO_2 (23, 24) suggest that the solubility of TiO_2 and ZrO_2 in monoclinic $NdO_{1.5}$ (stable at 1400–1500°C) is very limited. Thus, we have speculated that there is a very small region of solid solubility around $NdO_{1.5}$. At higher TiO_2 contents, the compounds Nd_2TiO_5 [orthorhombic (27)] and $Nd_2Ti_2O_7$ [monoclinic (28)] have been well characterized, and neither is known to show significant solid solution beyond their end-member compositions in the $NdO_{1.5}$–TiO_2–ZrO_2 system. At yet higher TiO_2 contents, two orthorhombic phases, $Nd_2Ti_4O_{11}$ and $Nd_4Ti_9O_{24}$, have been reported (29). Because of their similar symmetry and composition, we have assumed that these are two compositions within the solid solution range of a single phase. We further suggest a small solubility of ZrO_2 in this phase, and we have drawn a slightly wider two-phase region between it and $Nd_2Ti_2O_7$ than between the latter and Nd_2TiO_5.

A melt forms in the $NdO_{1.5}$–TiO_2 binary with a eutectic temperature at 1380°C and a composition of approximately 23 mol% $NdO_{1.5}$ and 77 mol% TiO_2 (22). At higher temperatures, the range of melt compositions widens, and this field is shown in Fig. 7. The ZrO_2 solubility in this melt has been drawn by analogy to the solubility of ZrO_2 in TiO_2 and, therefore, is speculative.

Because there is a paucity of data for the $NdO_{1.5}$–ZrO_2 join (23, 24), we complemented it with data from the $NdO_{1.5}$–HfO_2 system (25). These data are very similar to those for $NdO_{1.5}$–ZrO_2 because of the close chemical similarity and ionic radius (30) between zirconium and hafnium. The existence of the pyrochlore $Nd_2Zr_2O_7$ has been well established. Our own data, as well as those for the analogous $NdO_{1.5}$–HfO_2 system, suggest that significant solid solution from end-member $Nd_2Zr_2O_7$ toward both ZrO_2- and $NdO_{1.5}$-rich compositions occurs. A pyrochlore-type phase with the composition $Nd_{0.93}Zr_{2.8}O_7$ has been reported (24), and its existence was verified in the present work. Its synthesis represents a half-reversal limiting the maximum $NdO_{1.5}$ in the ZrO_2-rich limb of the pyrochlore one-phase region. After reaction of stoichiometric amounts of $NdO_{1.5}$ and ZrO_2 for approximately 3 days, a cubic pyrochlore-type compound, along with unreacted ZrO_2, was initially formed. After more reaction time, a single-phase product was eventually formed; it is reasonable to assume that the initial pyrochlore was more $NdO_{1.5}$-rich than the final product. Although the products were not chemically analyzed, such a compositional and phase change (two phases to one) would represent a half-reversal of the pyrochlore–ZrO_2 two-phase region.

There are three regions of solid solution along the TiO_2–ZrO_2 join. A considerable amount of TiO_2 is soluble in ZrO_2 (monoclinic), thus forming a large single-phase region. As there appears to be little solubility of $NdO_{1.5}$ in the hafnium analog of this phase, we suggest that there is also very slight solubility of $NdO_{1.5}$ in ZrO_2. A second solid solution series extends from the compound $ZrTiO_4$ (orthorhombic) to both more TiO_2-rich and ZrO_2-rich compositions. Here too we suggest that a few mole percent of $NdO_{1.5}$ are soluble in this phase. Lastly, there is approximately 10 mol% ZrO_2 soluble in TiO_2. Some solubility of $NdO_{1.5}$ in this phase is suggested on the basis of data for the $NdO_{1.5}$–TiO_2 join.

From the XRD results of the compositions noted in Fig. 7 and the data available from the $NdO_{1.5}$–TiO_2, $NdO_{1.5}$–ZrO_2, and TiO_2–ZrO_2 joins, we have tentatively proposed phase boundaries in the $NdO_{1.5}$–TiO_2–ZrO_2 ternary. Our work along the $Nd_2Zr_2O_7$–$Nd_2Ti_2O_7$, $Nd_2Zr_2O_7$–TiO_2, and $Nd_2Ti_2O_7$–ZrO_2 joins helped to identify compositions that formed single phases. This defined the large area of single-phase pyrochlore that was drawn to include the compound $Nd_{0.93}Zr_{2.8}O_7$. Compositions along the $Nd_2Zr_2O_7$–TiO_2 join that yielded two- and three-phase products were used to limit two and three-phase fields. For compositions from 0.56 to 1.5 mol TiO_2 per $Nd_2Zr_2O_7$, the XRD data indicated that pyrochlore and exsolved ZrO_2 were present. Most likely the phase exsolved was a ZrO_2 solid solution containing some TiO_2. Because no significant changes were noted in the XRD pattern of the ZrO_2 which in turn would have had little effect on the lattice parameter, the concentration of TiO_2 would have been low. Thus, the two-phase region in Fig. 7 was drawn to reflect this. Although XRD data for the composition 2 mol TiO_2 per mole of $Nd_2Zr_2O_7$ indicated that two phases (pyrochlore and ZrO_2 solid solution) were present, we elected to draw a three phase region around that composition. This is based on XRD results from several nearby compositions examined. The other phase present should be $Nd_2Ti_2O_7$. Its amount would be quite small, and it might not be detected by XRD because the main peak of $Nd_2Ti_2O_7$ is almost coincidental with that of the pyrochlore phase.

Our data on the $Nd_2Ti_2O_7$–ZrO_2 join indicated that a three-phase region existed at low ZrO_2 concentrations which is consistent with results from TiO_2-rich compositions along the $Nd_2Zr_2O_7$–TiO_2 join.

In another part of the ternary system, XRD data for the composition 55 mol% $NdO_{1.5}$, 10 mol% TiO_2, and 35 mol% ZrO_2 indicated that a pyrochlore-type compound was present along with Nd_2TiO_5, whereas more TiO_2-rich compositions (e.g., 47 mol% $NdO_{1.5}$, 32 mol% TiO_2, and 21 mol% ZrO_2) contained coexisting pyrochlore and $Nd_2Ti_2O_7$. These data were used to define the two-phase regions pyrochlore–Nd_2TiO_5 and pyrochlore–$Nd_2Ti_2O_7$ and the three-phase region pyrochlore–Nd_2TiO_5–$Nd_2Ti_2O_7$. Finally, as little information is available for the ternary system in the $NdO_{1.5}$-rich and TiO_2-rich regions, speculated phase boundaries, based on the phases in the binary systems, have been drawn.

It should be remembered that this phase diagram for the $NdO_{1.5}$–TiO_2–ZrO_2 ternary system, and thus some of the phase boundaries proposed here, is not exact.

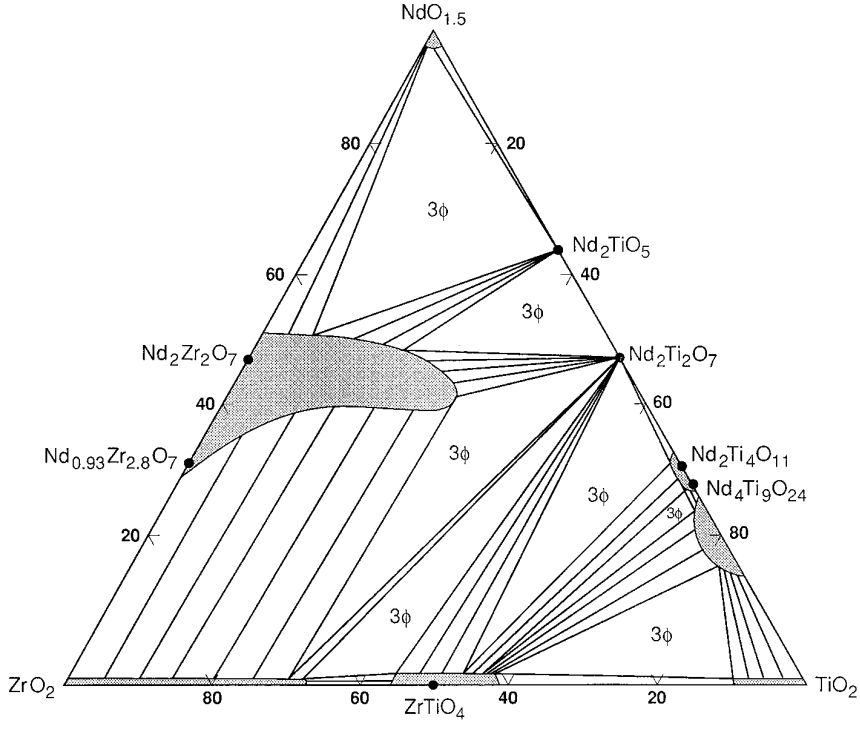

FIG. 7. Tentative phase diagram for $NdO_{1.5}$–TiO_2–ZrO_2 between 1400 and 1500°C. Shaded areas indicate regions of single-phase solid solution. Tie lines indicate two-phase regions. Unshaded, open areas indicate three phase regions (3ϕ).

Pyrochlore-Type Solid Solutions in the System $Ce_2Ti_2O_7$–$Ce_2Zr_2O_7$

The compound $Ce_2Zr_2O_7$ was prepared as shown in Eq. [1]. A mixture reacted at 1450°C in Ar–4% H_2 for a total of 40 h, with two regrindings, yielded a cubic pyrochlore-type compound with an X-ray powder pattern matching that reported for $Ce_2Zr_2O_7$ (31). Reacting this compound in flowing Ar without H_2 at 1350°C for an additional 30 h with three regrindings, however, caused a structural change from the ordered pyrochlore to a disordered defect fluorite structure. This is most likely due to small amounts of Ce(IV) formed from Ce(III) by traces of oxygen in the argon. This tentative conclusion is based on the fact that the ionic radius of Ce(IV) is similar to that of the heavy lanthanides, *Ln'*(III) (30), which form defect fluorite dizirconates.

A mixture with a composition equivalent to $2CeO_{1.5} \cdot 1.9ZrO_2 \cdot 0.1TiO_2$ also behaved differently according to the gaseous atmosphere used. In Ar–4% H_2 it yielded a pyrochlore-type compound, but unreacted ZrO_2 was also detected. Short reaction times (36 h with two regrindings) in Ar at 1200°C resulted in more than one phase, whereas additional reaction at 1350°C and regrinding resulted in the formation of a defect fluorite compound. As the titanium content was increased to $1.9TiO_2$, preparations reacted in Ar–4% H_2 at 1450°C yielded multiple products including a phase similar to the perovskite-type phase $Ce_2O_3 \cdot (3TiO_{2-m})$, which suggests that reduction of the titanium occurred. Heating one of these preparations in Ar resulted in the formation of $Ce_2Ti_2O_7$ and at least one additional minor cubic phase. Identifying this cubic phase without ambiguity as pyrochlore-type or fluorite was not possible because of the presence of numerous, more intense lines from $Ce_2Ti_2O_7$.

Substitution of Zirconium for Titanium in the Perovskite-Type Phases $SrNd_2Ti_4O_{12}$ and $Sr_2Ce_2Ti_5O_{16}$

The formation of perovskite-type solid solutions in the series $Sr_{4-x}Ln_{2x/3}Ti_4O_{12}$ (Ln = La–Nd, $0 \le x \le 4$), where the lanthanide ion is trivalent (8), and $Sr_{6-12x}Ce_{6x}Ti_5O_{16}$ ($0.08 \le x \le 0.43$), where cerium is tetravalent (9), has been previously studied. Perovskite-type solid solutions also have been reported in the system $Na_{0.5}La_{0.5}Ti_{1-x}Zr_xO_3$ ($Na_2La_2Ti_{4-y}Zr_yO_{12}$, $y = 4x$) at all compositions examined (10). This is similar to the series $Sr_{4-x}Ln_{2x/3}Ti_4O_{12}$, where $x = 3$ with partial substitution of the titanium with zirconium and two sodiums replacing one strontium and a vacancy. Thus, attempts were made to prepare perovskite-type solid solutions of the type $SrNd_2Ti_{4-y}Zr_yO_{12}$ ($y = 0.2$, 0.4, 0.8, 1.2, or 4.0) and $Sr_2Ce_2Ti_{5-y}Zr_yO_{16}$ ($y = 0.25$, 0.5, 1.0, 1.5, or 5.0), but no single-phase products were obtained for any composition.

Some single-phase solid solution formation had been expected in the above system based on the behavior of the series $Na_2La_2Ti_{4-y}Zr_yO_{12}$ where single-phase solid solution formation was reported at any composition (10). Our reexamination of the data indicates that only at $y = 0.4$ was a single-phase, perovskite-type solid solution formed. As the amount of zirconium substituted for titanium increased, the number of diffraction lines increased, and lines consistent with the pyrochlore $La_2Zr_2O_7$ appeared. This suggests that in the series $Na_2La_2Ti_{4-y}Zr_yO_{12}$ single-phase, perovskite-type solid solutions only occur at low concentrations of zirconium.

CONCLUSIONS

The formation of pyrochlore-type solid solutions between several dititanates and dizirconates has been investigated. Complete solubility was found in the pyrochlore–pyrochlore-type systems $Er_2Ti_2O_7$–$Nd_2Zr_2O_7$ and $Nd_{1.2}Er_{0.8}Ti_2O_7$–$Nd_2Zr_2O_7$. Partial solubility of $Nd_2Ti_2O_7$ having a monoclinic structure in defect fluorite $Er_2Zr_2O_7$ was observed to form a pyrochlore-type phase at intermediate compositions. While only the pyrochlore-type phase was detected in the XRD data, the system did not appear to obey Vegard's law.

In the $NdO_{1.5}$–TiO_2–ZrO_2 system, it was determined that there was partial solubility of $Nd_2Ti_2O_7$ in $Nd_2Zr_2O_7$. Pyrochlore-type solid solutions, which have the composition $Nd_2Zr_{2-x}Ti_xO_7$, were found to exist up to approximately $x = 0.86$, at which point the solid solution became saturated and a monoclinic phase, in addition to the pyrochlore, was detected. The systems $Nd_2Zr_2O_7$–TiO_2 and $Nd_2Ti_2O_7$–ZrO_2 were investigated to help define a region of pyrochlore solid solution formation in the system $NdO_{1.5}$–TiO_2–ZrO_2. A tentative phase diagram for the system $NdO_{1.5}$–TiO_2–ZrO_2 between 1400 and 1500°C was proposed based on the results discussed here and those reported for previously studied joins. Information from the $NdO_{1.5}$–HfO_2 join (25) was used to complement the previously reported data for the $NdO_{1.5}$–ZrO_2 join; however, the pyrochlore solid solution region in the phase diagram for $NdO_{1.5}$–HfO_2 does not extend to the composition $Nd_{0.93}Hf_{2.8}O_7$. The data presented for the $NdO_{1.5}$–ZrO_2 system here and in previous studies (23, 24), however, suggest that $Nd_{0.93}Hf_{2.8}O_7$ should exist within the pyrochlore solid solution series.

Attempts at solid solution formation between $Ce_2Ti_2O_7$ and $Ce_2Zr_2O_7$ were not successful because of the experimental difficulties in maintaining cerium as Ce(III) and titanium as Ti(IV) while allowing sufficient time for equilibration.

Attempts to replace titanium with zirconium in the perovskite-type phases $SrLn_2Ti_4O_{12}$ and $Sr_2Ce_2Ti_5O_{16}$ were not successful.

The solubility of a solid solution, representative of the

systems studied here, in several leachants, including the WIPP ''A'' brine (32), will be reported in another publication along with results from related compounds (33). The studies performed suggest that some of the titanates and zirconotitanates may be good candidates for stabilizing trivalent actinide elements.

ACKNOWLEDGMENTS

This research was supported by the Division of Materials Sciences, Office of Basic Energy Sciences, U.S. Department of Energy, under Contract DE-AC05–96OR22464 and performed at the Oak Ridge National Laboratory managed by Lockheed Martin Energy Research Corporation. S.S.S. is grateful for the support by the Division of Chemical Sciences, Office of Basic Energy Sciences, U.S. Department of Energy, under Grant DE-FG05–88ER13865 to the University of Tennessee, Knoxville.

REFERENCES

1. M. Gasperin, *Acta Crystallogr. B* **31,** 2129 (1975).
2. M. A. Subramanian, G. Aravamudan, and G. V. Subba Rao, *Prog. Solid State Chem.* **15,** 55 (1983).
3. M. A. Subramanian and A. W. Sleight, *in* ''The Handbook on the Physics and Chemistry of the Rare Earths'' (K. A. Gschneidner, Jr., and L. Eyring, Eds.), p. 225. Elsevier Science, Amsterdam, 1993.
4. C. E. Bamberger, H. W. Dunn, G. M. Begun, and S. A. Landry, *J. Less-Common Met.* **109,** 209 (1985).
5. C. E. Bamberger, T. J. Haverlock, S. S. Shoup, O. C. Kopp, and N. A. Stump, *J. Alloys Compounds* **204,** 101 (1994).
6. P. K. Moon and H. L. Tuller, *Solid State Ionics* **28–30,** 470 (1988).
7. C. Heremans, B. J. Wuensch, J. K. Stalick, and E. Prince, *J. Solid State Chem.* **117,** 108 (1995).
8. S. S. Shoup, T. J. Haverlock, and C. E. Bamberger, *J. Am. Ceram. Soc.* **78,** 1261 (1995).
9. C. E. Bamberger, T. J. Haverlock, and O. C. Kopp, *J. Am. Ceram. Soc.* **77,** 1659 (1994).
10. A. G. Belous, G. N. Novitskaya, L. G. Gavrilova, S. V. Polyanetskaya, and Z. Ya. Makarova, *Ukrain. Khim. Zh.* (*Russ. Ed.*) **51,** 13 (1985).
11. J. Bouwma, K. J. de Vries, and A. J. Burggraaf, *Phys. Status Solidi A* **35,** 281 (1976).
12. R. C. Ewing, W. Lutze, and W. J. Weber, *J. Mater. Res.* **10,** 243 (1995).
13. A. E. Ringwood, S. E. Kesson, N. G. Ware, W. Hibberson, and A. Major, *Nature* **278,** 219 (1979).
14. A. E. Ringwood, ''Safe Disposal of High Level Nuclear Reactor Wastes: A New Strategy.'' Australia National Univ. Press, Canberra, 1978.
15. E. R. Vance, *Mater. Res. Soc. Bull.* **19,** 28 (1994).
16. E. R. Vance, P. J. Angel, B. D. Begg, and R. A. Day, *in* ''Scientific Basis for Nuclear Waste Management XV, Mater. Res. Soc. Symp. Proc. Vol. 333,'' (R. C. Ewing, Ed.), p. 293. Materials Research Society, Pittsburgh, PA, 1994.
17. T. J. White and J. Mitamura, in ''Scientific Basis for Nuclear Waste Management XVI, Mater. Res. Soc. Symp. Proc. Vol. 294'' (C. G. Interrante and R. T. Pabalan, Eds.), p. 109. Materials Research Society, Pittsburgh, PA, 1993.
18. I. Hayakawa and H. Kamizono, *J. Mater. Sci.* **28,** 513 (1993).
19. W. A. Deer, R. A. Howie, and J. Zussman, ''Rock-Forming Minerals,'' Vol. 1A: ''Orthosilicates,'' 2nd ed., p. 418. Longman Group, New York, 1982.
20. B. C. Chakoumakos and R. C. Ewing, *in* ''Scientific Basis for Nuclear Waste Management VIII, Mater. Res. Soc. Symp. Proc. Vol. 44'' (C. M. Jantzen, J. A. Stone, and R. C. Ewing, Eds.), p. 641, Materials Research Society, Pittsburgh, PA, 1985.
21. E. Specht, unpublished program, Metals and Ceramics Division, Oak Ridge National Laboratory, Oak Ridge, TN, 1995.
22. G. A. Teterin, V. F. Zinchenko, A. V. Zagorodnyuk, and I. M. Minaev, *Sov. Progr. Chem.* (*Engl. Transl.*), **54,** 31 (1988).
23. R. S. Roth, *J. Res. Natl. Bur. Stand.*, **56,** 17 (1956).
24. ''Powder Diffraction File,'' Card No. 28-679. Joint Committee for Powder Diffraction Standards, Swarthmore, PA, 1978.
25. A. V. Shevchenko, L. M. Lopato, and Z. A. Zaitseva, *Inorg. Mater.* **20,** 1316 (1985).
26. A. E. McHale and R. S. Roth, *J. Am. Ceram. Soc.* **69,** 827 (1986).
27. ''Powder Diffraction File,'' Card No. 33-0944. Joint Committee for Powder Diffraction Standards, Swarthmore, PA, 1983.
28. ''Powder Diffraction File,'' Card No. 33-0942. Joint Committee for Powder Diffraction Standards, Swarthmore, PA, 1983.
29. ''Powder Diffraction File,'' Card Nos. 32-684 and 33-0943. Joint Committee for Powder Diffraction Standards, Swarthmore, PA, 1982/1983.
30. R. D. Shannon, *Acta Crystallogr. A* **32,** 751 (1976).
31. J. J. Casey, L. Katz, and W. C. Orr, *J. Am. Chem. Soc.* **77,** 2187 (1955).
32. R. G. Dosch and A. W. Lynch, ''Interaction of Radionuclides with Geomedia Associated with the Waste Isolation Pilot Plant Site in New Mexico,'' SAND78–0297 (1978).
33. S. S. Shoup, C. E. Bamberger, T. J. Haverlock, and J. R. Peterson, *J. Nucl. Mater.,* in press.